

Spin dependent charge pumping in SiC metal-oxide-semiconductor field-effect-transistors

B. C. Bittel, P. M. Lenahan, J. T. Ryan, J. Fronheiser, and A. J. Lelis

Citation: [Applied Physics Letters](#) **99**, 083504 (2011); doi: 10.1063/1.3630024

View online: <http://dx.doi.org/10.1063/1.3630024>

View Table of Contents: <http://scitation.aip.org/content/aip/journal/apl/99/8?ver=pdfcov>

Published by the [AIP Publishing](#)

Articles you may be interested in

[Systematic investigation on in-plane anisotropy of surface and buried channel mobility of metal-oxide-semiconductor field-effect-transistors on Si-, a-, and m-face 4H-SiC](#)

Appl. Phys. Lett. **106**, 103506 (2015); 10.1063/1.4914385

[Electrically detected magnetic resonance study of defects created by hot carrier stress at the SiC/SiO₂ interface of a SiC n-channel metal-oxide-semiconductor field-effect transistor](#)

Appl. Phys. Lett. **105**, 043506 (2014); 10.1063/1.4891847

[An electrically detected magnetic resonance study of performance limiting defects in SiC metal oxide semiconductor field effect transistors](#)

J. Appl. Phys. **109**, 014506 (2011); 10.1063/1.3530600

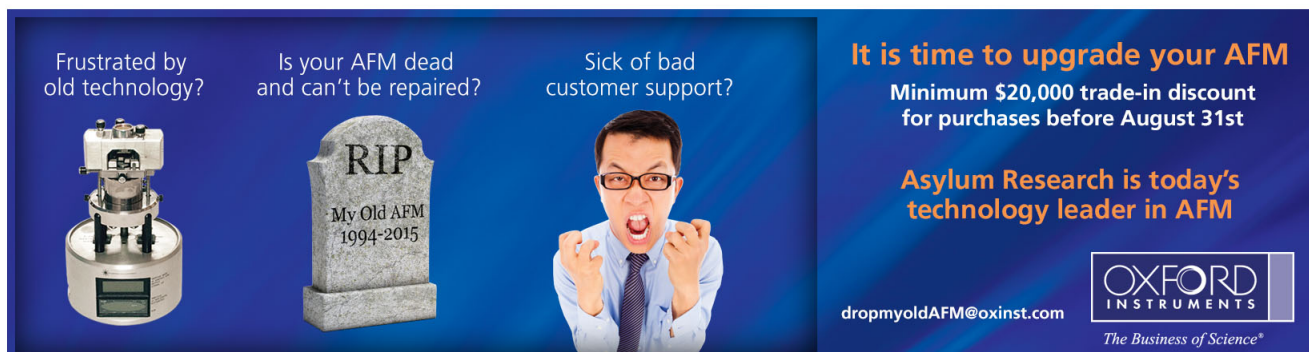
[Correlation between channel mobility and shallow interface traps in SiC metal-oxide-semiconductor field-effect transistors](#)

J. Appl. Phys. **92**, 6230 (2002); 10.1063/1.1513210

[Relationship between channel mobility and interface state density in SiC metal-oxide-semiconductor field-effect transistor](#)

J. Appl. Phys. **91**, 1568 (2002); 10.1063/1.1428085


Frustrated by old technology? Is your AFM dead and can't be repaired? Sick of bad customer support?



It is time to upgrade your AFM
Minimum \$20,000 trade-in discount for purchases before August 31st

Asylum Research is today's technology leader in AFM

dropmyoldAFM@oxinst.com



The Business of Science®

Spin dependent charge pumping in SiC metal-oxide-semiconductor field-effect-transistors

B. C. Bittel,^{1,a)} P. M. Lenahan,¹ J. T. Ryan,² J. Fronheiser,³ and A. J. Lelis⁴

¹The Pennsylvania State University, University Park, Pennsylvania 16802, USA

²National Institute of Standards and Technology, Semiconductor Electronics Division, 100 Bureau Drive, Gaithersburg, Maryland 20899, USA

³GE Global Research, 1 Research Circle, Niskayuna, New York 12309, USA

⁴US Army Research Laboratory, 2800 Powder Mill Rd, Adelphi, Maryland 20783, USA

(Received 14 June 2011; accepted 5 August 2011; published online 25 August 2011)

We demonstrate a very powerful electrically detected magnetic resonance (EDMR) technique, spin dependent charge pumping (SDCP) and apply it to 4H SiC metal-oxide-semiconductor field-effect-transistors. SDCP combines a widely used electrical characterization tool with the most powerful analytical technique for providing atomic scale structure of point defects in electronic materials. SDCP offers a large improvement in sensitivity over the previously established EDMR technique called spin dependent recombination, offering higher sensitivity and accessing a wider energy range within the bandgap. © 2011 American Institute of Physics. [doi:10.1063/1.3630024]

Charge pumping is widely utilized to characterize interface/near interface defects in metal-oxide-semiconductor field-effect-transistors (MOSFETs).¹⁻³ It provides detailed information about the purely “electronic” aspects of defects but it does not provide information about atomic scale structure.¹⁻³ Conventional electron paramagnetic resonance (EPR) has unrivaled analytical power to identify atomic scale structure of defect centers but does not provide a direct connection between the defect structure and electronic properties.⁴ Conventional EPR is limited in transistor studies because its sensitivity is of order 10^{10} defects, a number significantly larger than the total number of electrically active defects in most transistors. The limitations of conventional EPR are, to some extent, ameliorated by electrically detected magnetic resonance (EDMR); a variety of EDMR related techniques have been demonstrated to be quite useful in various circumstances.⁵⁻⁷ In semiconductor device research, spin dependent recombination (SDR) has been quite useful.⁶⁻⁹ SDR exploits the fact that the capture of charge carriers at paramagnetic deep level defects is spin dependent; it allows resonance measurements in transistors and other solid state devices.⁶⁻⁹ We show that spin dependent charge pumping (SDCP) can be a powerful vehicle for EDMR. It exploits the same spin dependent charge capture process as SDR, but offers substantial advantages in both sensitivity and the range of accessible energy. We apply SDCP to a topic of substantial current interest: performance limiting defects in SiC MOSFETs.

Silicon carbide (SiC) is a promising wide band gap semiconductor for high power and high temperature applications. The 4H SiC polytype is arguably the most promising. The performance of 4H silicon carbide MOSFETs is limited by poorly understood defects in the interface/near interface region between the silicon carbide and silicon dioxide,¹⁰⁻¹² which results in poor channel mobility and large threshold voltage instabilities.¹⁰⁻¹² Previous SDR measurements identified defects in SiC MOSFETs; the most commonly observed

defect spectrum has an isotropic $g = 2.0030 \pm 0.0003$ and has been tentatively assigned to a silicon vacancy.^{6,7} (In the simplest case, the EPR condition is given by $h\nu = g\beta H$, where h is Planck’s constant, β is the Bohr magneton, ν is the frequency of the microwave radiation, and H is the magnetic field at resonance.⁴ The g is essentially a second-rank tensor.)

We apply SDCP to SiC lateral n-channel MOSFETs with dimensions of $1000 \mu\text{m} \times 2 \mu\text{m}$ and a 50 nm thick gate oxide. This device has an interface trap density of order $4 \times 10^{11} \text{ cm}^{-2}$ determined from the charge pumping measurements. The SDCP measurements were carried out at room temperature utilizing a custom built spectrometer consisting of a resonance instrument 8330 series X-band microwave bridge with a transverse electric 102 microwave cavity and an electromagnet controlled by a custom-built magnetic-field controller. The magnetic field was calibrated using a strong pitch standard with conventional EPR. To perform SDCP, we applied 1 V to the shorted source drain and body contacts while applying an approximately square waveform to the gate. Measurements involve charge pumping frequencies from 4 kHz to 1 MHz with rise and fall times of 20 ns and 50% duty cycle. SDCP detection is accomplished by monitoring the substrate current utilizing a lock-in amplifier with a modulation frequency of 1 kHz in all measurements.

Figure 1 illustrates a comparison between SDR and 1 MHz SDCP spectra taken at the maximum microwave power level of 150 mW with the crystalline c-axis orientated almost parallel to the applied magnetic field. In both SDCP and SDR measurements, parameters were chosen to optimize signal to noise. SDCP measurements were taken with a constant base level gate pulse of -6 V and a high level of 1 V . The SDCP yields an isotropic spectrum with $g = 2.0035 \pm 0.0003$ and a 13 G linewidth. In the SDR measurement, the source-drain to substrate bias was 2.35 V with 0 V applied to the gate. A schematic comparison of SDR and SDCP is shown on the right of Figure 1. Whereas in SDR, a constant DC bias is applied to the gate and in SDCP, a square wave is applied to the gate. Note that, taking into account the large difference in signal averaging times, the difference in

^{a)} Author to whom correspondence should be addressed. Electronic mail: bcb183@psu.edu.

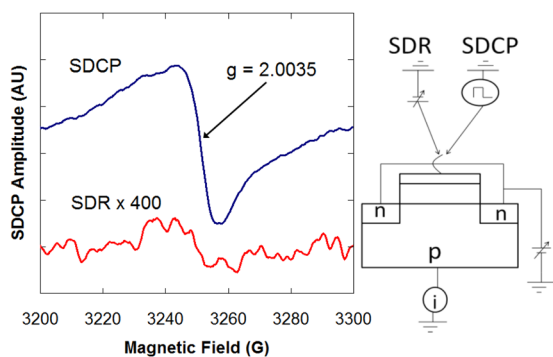


FIG. 1. (Color online) (Left) SDCP and SDR comparison with the SiC crystalline c-axis almost parallel to the applied magnetic field and with biasing optimized in each case for the best signal to noise ratio. The SDCP trace has a signal to noise ratio of approximately 500 after 1000 s of signal averaging. The SDR spectrum has a signal to noise ratio of approximately 4 after 60 000 s of signal averaging. (The SDR trace amplitude is multiplied by 400 to be visible on the graph). This result demonstrates a sensitivity increase of approximately 1000 with SDCP compared to SDR, as signal to noise ratio increases with the square root of time. (Curves are offset for clarity). (Right) Also shown is a schematic comparison of SDR and SDCP. In SDCP, a waveform generator is connected to the gate, while in SDR a constant dc voltage is applied to the gate. In both cases, the source and drain are tied together. They are forward biased for SDR and reversed biased for SDCP. In both cases, the substrate current is monitored.

sensitivity is about a factor of 1000. There are at least two reasons for this very large enhancement in sensitivity.

The charge pumping energy range is described by² the following expression:

$$\Delta E_{CP} = 2k_B T \ln\left(\frac{\Delta V_G}{v_{th} \sigma n_i \sqrt{t_r t_f} (V_{th} - V_{fb})}\right). \quad (1)$$

Here, ΔV_G is the gate voltage sweep range = 7 V, v_{th} is the thermal drift velocity = 1.25×10^7 cm s⁻¹, σ is the capture cross section taken to be 1×10^{-16} cm², n_i is the intrinsic carrier concentration = 5×10^{-9} cm⁻³, t_r and t_f are the rise and fall times, and both 20 ns and $V_{th} - V_{fb}$ is the threshold voltage minus the flatband voltage = 7V. Expression (1) yields an ΔE_{cp} of 2.9 eV for our measurements, nearly all of the 3.26 eV bandgap of SiC. SDR, however, is only sensitive to the energy range covered by the gated diode recombination current, that is $\frac{1}{2}q|V_f|$,^{13,14} where q is the electronic charge and V_f is the source drain to substrate forward bias. In this case, $|V_f|$ is 2.35 V, yielding an energy range of 1.2 eV. Thus, with parameters optimized for both measurements, SDCP is sensitive to almost three times the energy range of the SDR measurement.

A large additional increase in sensitivity results from the fact that in SDCP, the traps are accessed at a frequency of up to 1 MHz (the charge pumping frequency) whereas in SDR, the access rate is controlled by the steady state rate of charge carrier capture. The capture rate is approximately given by $\sigma v_{th} n$,¹⁵ where n is the density of charge carriers, σ is the capture cross section, and v_{th} is the thermal drift velocity. Assuming a capture cross section of 1×10^{-16} cm², thermal drift velocity of 1.25×10^7 cm s⁻¹ and a charge carrier concentration, for $|V_f|$ of 2.35 V, of $n = n_i^{q|V_f|/2kT} = 4.3 \times 10^{11}$ cm⁻³, the capture rate is approximately 500 Hz. Thus, for 1 MHz charge pumping frequency, SDCP accesses the paramagnetic defect centers about 2000 times more frequently

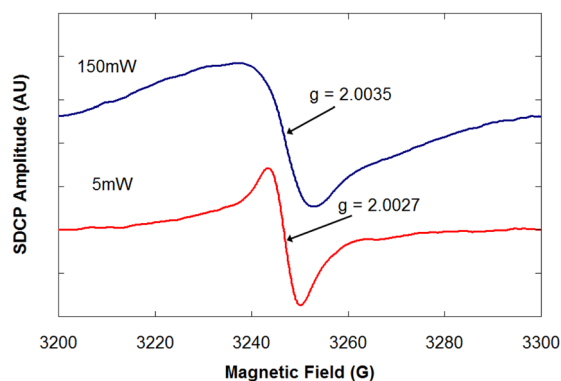


FIG. 2. (Color online) SDCP amplitude at two different microwave powers with the SiC crystalline c-axis almost parallel to the applied magnetic field. Note the difference in line width (13 and 7 G) and g-value (2.0035 and 2.0027) between 150 mW and 5 mW, respectively. (Curves are offset for clarity).

than SDR. Our experiment results indicate that the wider range of energy explored and higher rate of defect centers accessed combines to yield an increase in signal to noise of about a factor of 1000.

Figure 2 illustrates 1 MHz SDCP traces with the magnetic field parallel to the surface normal at two levels of microwave power, 150 mW and 5 mW, also taken with a constant base level of -6 V and a high level of 1 V with rise and fall times of 20 ns. Note, the much narrower linewidth and the slightly different zero crossing g values (2.0027 ± 0.0003 versus 2.0035 ± 0.0003) at 5 mW. The lower power SDCP trace linewidth and g-value of 2.0027 closely match the SDR/EDMR results on similar devices.^{6,7} As discussed previously, the narrow 2.0027 SDR spectrum has been linked to a silicon vacancy or similar defect structure.^{6,7} Although we are unable to provide definitive identification of the broad EDMR spectrum with $g = 2.0035$, we note that the spectrum has extended shoulders and does not closely resemble any of the commonly observed defect EPR patterns in 4H SiC.¹⁶ Rather, broad featureless spectra have been observed with both conventional EPR and EDMR in another system, amorphous hydrogenated silicon, where they have been associated with “band tail” states.¹⁷ We tentatively ascribe this wide spectrum to some involvement with such states.

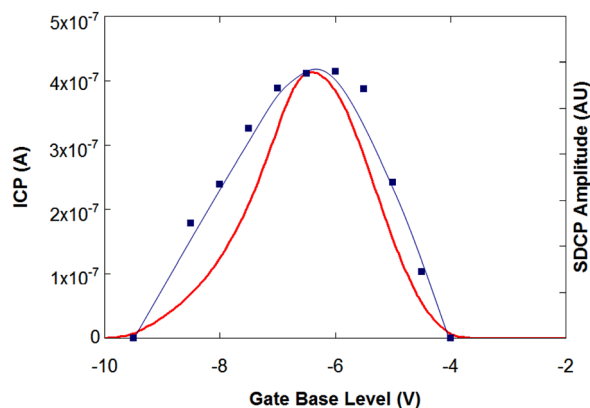


FIG. 3. (Color online) SDCP amplitude (blue squares and line to guide the eye) and charge pumping current (red line) plotted against base level gate voltage, with constant amplitude of 8 V with 1 MHz pulse frequency and rise and fall times of 20 ns.

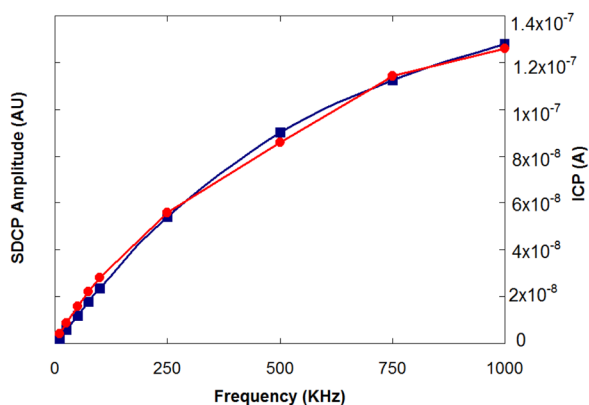


FIG. 4. (Color online) SDCP amplitude (blue squares and line) and charge pumping current (red circles and line) versus charge pumping frequency with base level of -6 V, high level of 1 V, and rise and fall times of 20 ns.

Figure 3 compares the SDCP amplitude and charge pumping current with constant amplitude gate pulses of 8 V, and varying base level gate voltages at 1 MHz with rise and fall times of 20 ns. Figure 4 compares SDCP amplitude and charge pumping current versus frequency with constant base voltage of -6 V and high level voltage of 1 V at 1 MHz with rise and fall times of 20 ns. The close similarity between the charge pumping and SDCP results of Figures 3 and 4 suggests that the defects observed in SDCP are dominating deep levels in the interface/near interface region.

Our results demonstrate that SDCP offers sensitivity of several orders of magnitude above SDR and accesses a wider range of the band gap. SDCP also provides a straight forward link between the widely utilized charge pumping measurements and the analytical power of magnetic resonance.

We wish to thank Thomas Aichinger for assistance in setting up the electrical measurement apparatus. The work at Penn State supported by the U.S. Department of Commerce under Award No. NIST 60NANB10D109 and the US Army Research Laboratory. Any opinions, findings, conclusions, or other recommendations expressed herein are those of the authors and do not necessarily reflect the views of the U.S. Commerce Department or the US Army Research Laboratory.

¹J. S. Brugler and P. G. A. Jespers, *IEEE Trans. Electron Devices* **ED-16**, 297 (1969).

²G. Groeseneken, H. E. Maes, N. Beltran, and R. F. Dekeersmaecker, *IEEE Trans. Electron Devices* **ED-31**, 42 (1984).

³D. B. Habersat, A. J. Lelis, J. M. McGarrity, F. B. McLean, and S. Potbhare, *Mater. Sci. Forum* **600**, 743 (2009).

⁴J. A. Weil, J. R. Bolton, and J. E. Wertz, *Electron Paramagnetic Resonance* (Wiley, New York, 1994).

⁵M. V. Costache, M. Sladkov, S. M. Watts, C. H. van der Wal, and B. J. van Wees, *Phys. Rev. Lett.* **97**, 216603 (2006).

⁶C. J. Cochrane, P. M. Lenahan, and A. J. Lelis, *J. Appl. Phys.* **109**, 014506 (2011).

⁷D. J. Meyer, N. A. Bohna, P. M. Lenahan, and A. J. Lelis, *Appl. Phys. Lett.* **84**, 3406 (2004).

⁸D. J. Lepine, *Phys. Rev. B* **6**, 2 (1972).

⁹D. Kaplan, I. Solomon, and N. F. Mott, *J. Phys. Lett.* **39**, 15 (1978).

¹⁰J. A. Cooper, *IEEE Trans. Electron Devices* **49**, 4 (2002).

¹¹A. J. Lelis, D. Habersat, R. Green, A. Ogunniyi, M. Gurfinkel, J. Suehle, and N. Goldsman, *IEEE Trans. Electron Devices* **55**, 8 (2008).

¹²A. J. Lelis, D. Habersat, R. Green, and N. Goldsman, *Mater. Sci. Forum* **600**, 807 (2009).

¹³M. A. Jupina and P. M. Lenahan, *IEEE Trans. Nucl. Sci.* **36**, 1800 (1989).

¹⁴D. J. Fitzgerald and A. S. Grove, *Surf. Sci.* **9**, 347 (1968).

¹⁵D. K. Schroder, *Semiconductor Material and Device Characterization*, 3rd ed. (Wiley, Hoboken, New Jersey, 2006).

¹⁶J. I. Soya, T. Umeda, N. Mizuochi, N. T. Son, E. Janzen, and T. Ohshima, *Phys. Status Solidi B* **245**, 1298 (2008).

¹⁷H. Dersch, L. Schweitzer, and J. Stuke, *Phys. Rev. B* **28**, 4678 (1983).